J|A|C|S COMMUNICATIONS

Published on Web 12/19/2008

Synthesis of Uniform Ferrimagnetic Magnetite Nanocubes

Dokyoon Kim, Nohyun Lee, Mihyun Park, Byung Hyo Kim, Kwangjin An, and Taeghwan Hyeon*

National Creative Research Initiative Center for Oxide Nanocrystalline Materials and School of Chemical and Biological Engineering, Seoul National University, Seoul 151-744, Korea

Received November 5, 2008; E-mail: thyeon@snu.ac.kr

Nanoparticles have been intensively studied due to their potential applications as well as their fundamental size-dependent properties.[1] For many of these applications, the synthesis of uniform nanoparticles is of key importance because the electrical, optical, and magnetic properties of the nanoparticles are strongly dependent on their dimensions.[1] Over the past decade, uniform nanoparticles with various compositions, sizes, and shapes have been synthesized using several different methods including hot-injection and heat-up processes.[1,2] Among various nanoparticles, magnetic nanoparticles have attracted significant attention for many technological applications including magnetic resonance imaging contrast agents, magnetic carriers for drug delivery systems, biosensors, and bioseparation.[3] Although ferri- or ferromagnetic nanoparticles are desirable for many of these applications, superparamagnetic nanoparticles of <30 nm have generally been used because nearly no preparation method is available for the synthesis of uniform ferrimagnetic nanoparticles larger than 30 nm. Interestingly, magnetosomes in magnetotactic bacteria are composed of single-domain magnetite nanocrystals in the 30−100 nm range and often with cube or cuboctahedron shapes.[4] These magnetosomes have attracted a lot of attention because of their biotechnological applications derived from their narrow size and shape distribution and inherent biocompatibility. In our continuous effort to improve the synthesis of magnetic nanoparticles,[5] we herein report on the synthesis of uniform magnetite (Fe_3O_4) nanocubes ranging in size from 20 to 160 nm.

In a typical synthesis, iron(III) acetylacetonate (0.71 g) was added to a mixture of oleic acid (1.13 g) and benzyl ether (10.4 g). The mixture solution was degassed at room temperature for 1 h and then heated to 290 °C at the rate 20 °C/min under vigorous magnetic stirring. The reaction mixture was maintained at this temperature for 30 min. After cooling to room temperature, a mixture of toluene and hexane was added to the solution. The solution was then centrifuged to precipitate the Fe_3O_4 nanocubes. The separated precipitate was washed using chloroform. The TEM image (Figure 1a) revealed that the synthesized nanocubes have a uniform edge length of 79 nm (78.5 nm ± 6.9 nm). The high-resolution TEM (HRTEM) image showed the highly crystalline nature of the nanocubes (inset of Figure 1a), and the measured *d*-spacing value (4.18 Å) was twice the value of the magnetite (400) plane. The X-ray diffraction pattern clearly indicated that the synthesized nanocubes are magnetite (Fe_3O_4) rather than similarly structured maghemite (γ-Fe_2O_3) (Figure S1).[5a]

The dimensions of the nanocubes could be controlled by varying the experimental conditions. For example, when the amount of benzyl ether was reduced to 5.2 g and the reaction time was increased to 1 h, ~110-nm-sized particles composed of truncated cubes and truncated octahedra were obtained (Figure 1b). By increasing the reaction time to 1.5 and 2 h, the particles grew to a larger and more perfect cubic shape with edge dimensions of 150 nm (Figure 1c) and 160 nm (Figure 1d), respectively. Based on

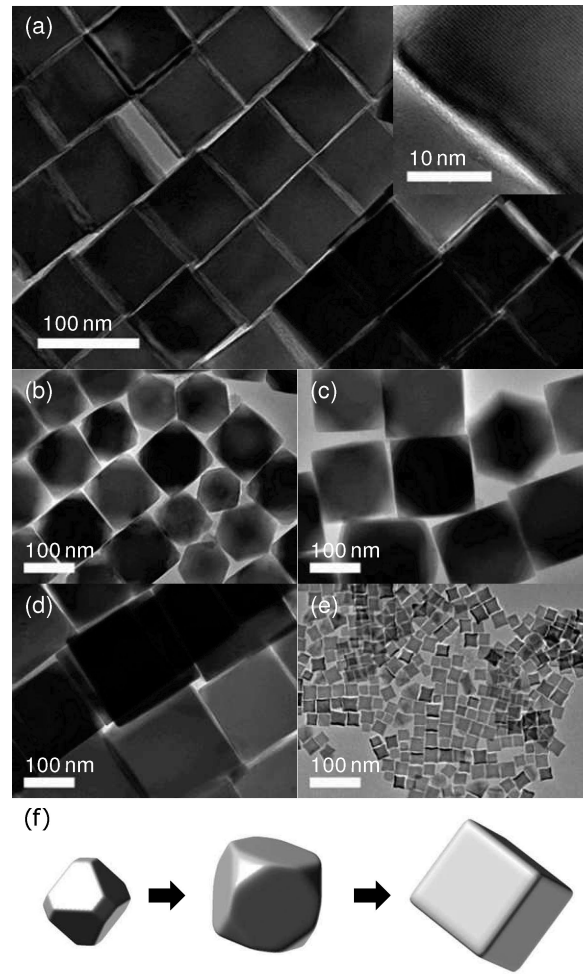

Figure 1. TEM images of (a) 79-nm-sized Fe_3O_4 nanocubes (inset: HRTEM image); (b) mixture of truncated cubic and truncated octahedral nanoparticles with an average dimension of 110 nm; (c) 150-nm-sized truncated nanocubes; (d) 160-nm-sized nanocubes; (e) 22-nm-sized nanocubes. (f) Schematics showing the overall shape evolution of the Fe_3O_4 nanoparticles.

the HRTEM study, we concluded that the nanocubes are formed as a result of fast growth along ⟨111⟩ directions, and the surfaces of the final nanocubes correspond to {100} planes, which is similar to the magnetite nanocrystals found in magnetotactic bacteria.[4] The overall shape evolution is illustrated in Figure 1f. Kinetically controlled growth under high monomer concentration seems to be responsible for this anisotropic growth.[2a] When 0.40 g of 4-biphenylcarboxylic acid and 1.27 g of oleic acid were used, while keeping all the other reaction conditions the same for the synthesis of 79-nm-sized nanocubes, smaller 22-nm-sized nanocubes were synthesized (Figure 1e and Figure S2).

10.1021/ja8086906 CCC: $40.75

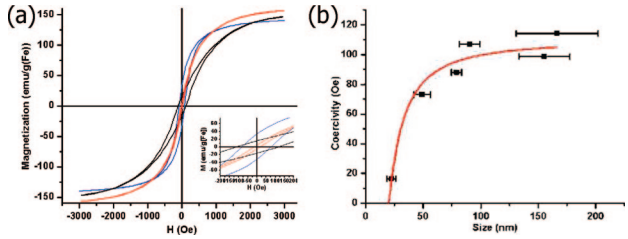

Figure 2. Magnetic behavior of the Fe_3O_4 nanocubes measured at 300 K: (a) M−H curves for 22-nm- (red), 80-nm- (blue), and 160-nm- (black) sized nanocubes; (b) size-dependent coercivity (error bar: size distribution).

The current synthetic process is relatively easy to scale up.[5a] For example, when the reaction size for the synthesis of 79-nm-sized nanocubes was increased by a factor of 10, 1.6 g of the nanocubes with an edge length of 49 nm were obtained (Figure S3). Recently, Yang and co-workers synthesized uniform magnetite nanocubes with sizes ranging from 6.5 to 30 nm from thermal reaction of $Fe(acac)_3$ in a mixture of 1,2-hexadecandiol, oleic acid, oleylamine, and benzyl ether.[6a] Chen and co-workers synthesized relatively uniform 50-nm-sized magnetite nanocubes from a solvothermal reaction of ferrocene with H_2O_2 in a mixture containing polyvinylpyrrolidone, water, and alcohol.[6b]

The synthesized Fe_3O_4 nanocubes are a soft ferrimagnetic material with high saturation magnetization and low coercivity. Figure 2 shows the magnetic behavior of the nanocubes measured at 300 K. All the samples showed hysteresis loops in the M−H curves, indicating the ferrimagnetic nature of the Fe_3O_4 nanocubes (Figure 2a). The coercivities of various nanocube sizes are plotted in Figure 2b. In general, the coercivity of the superparamagnetic nanoparticles is zero above the blocking temperature. As the particle size increases, the coercivity at a given temperature increases rapidly upon the size exceeding the superparamagnetic limit, saturates when the size approaches the single-domain limit, and gradually decreases to the bulk value upon passing the multidomain region (Figure S4).[1b,7] By fitting the measured coercivity to the single-domain particle model[1b] (trend line in Figure 2b), the superparamagnetic limit of ~20 nm was estimated, which is in reasonable accord with the previous reports.[8] Although the single-domain limit of 128 nm was estimated for Fe_3O_4 nanospheres,[1b] our nanocubes did not show any sign of coercivity decrease up to 160 nm. The shape anisotropy and the interaction between closely spaced nanocubes might be responsible for this increased critical size of the single domain particles,[4a] and more rigorous investigation should be conducted to achieve a comprehensive understanding of the results.

To explore the potential application of the nanocubes, we applied them to the separation of histidine-tagged proteins. Fractionation of biomolecules by exploiting their different affinities to metal ions was first introduced as the concept of immobilized metal ion affinity chromatography.[9] Intermediate transition metal ions such as Ni(II), Cu(II), and Zn(II) based on Pearson's hard and soft acid classification are often used for these applications.[9] The use of nickel nanoparticles or nickel-containing magnetic nanostructures was recently demonstrated.[10] In our experiments, we employed the as-synthesized nanocubes without any nickel incorporation. Following our previously reported procedures,[10a] 59% loading and 50% retrieval (84% release of the load) of histidine-tagged green fluorescent protein were observed (Figure 3 left). We believe that the loading capacity can be increased further after optimization because the highest protein adsorption on Fe(III) is reached at low pH (<6) and low ionic strength condition.[9b] In a control experiment, only a 13% decrease in the fluorescent emission intensity was observed for red-emitting Cy5-labeled normal mouse IgG without histidine-tag, indicating the limited extent of the binding (Figure 3 right).

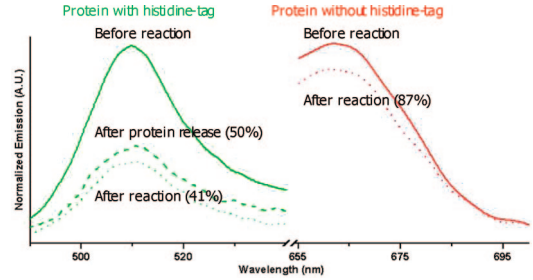

Figure 3. Fluorescence spectra showing the change of emission intensity before and after treating the solutions of histidine-tagged green fluorescent protein (green) or nonhistidine-tagged Cy5-labeled normal mouse IgG (red) with Fe_3O_4 nanocubes.

In summary, we synthesized uniform ferrimagnetic magnetite nanocubes in the size range from 20 to 160 nm. The magnetic behavior of the nanocubes was characterized, and magnetic separation of the histidine-tagged protein was demonstrated. These synthesized nanocubes are expected to find many applications where soft-magnet properties are useful.

Acknowledgment. The present work was supported by the KOSEF through the National Creative Research Initiative Program.

Supporting Information Available: Experimental procedures. TEM, XRD, and SQUID data. This material is available free of charge via the Internet at http://pubs.acs.org.

References

(1) (a) *The Chemistry of Nanostructured Materials*; Yang, P., Ed.; World Scientific Publishing: Singapore, 2003. (b) *Nanoscale Materials in Chemistry*; Klabunde, K. J., Ed.; Wiley-Interscience: New York, 2001. (c) *Nanoparticles*; Schmid, G., Ed.; Wiley-VCH: Weinheim, 2004. (d) *Semiconductor and Metal Nanocrystals*; Klimov, V. I., Ed.; Marcel Dekker, Inc.: New York, 2004.

(2) (a) Park, J.; Joo, J.; Kwon, S. G.; Jang, Y.; Hyeon, T. *Angew. Chem., Int. Ed.* **2007**, *46*, 4630–4660. (b) Donega, C. D.; Liljeroth, P.; Vanmaekelbergh, D. *Small* **2005**, *1*, 1152–1162.

(3) (a) Sun, S.; Murray, C. B.; Weller, D.; Folks, L.; Moser, A. *Science* **2000**, *287*, 1989–1992. (b) Hyeon, T. *Chem. Commun.* **2003**, 927–934. (c) Gu, H.; Xu, K.; Xu, C.; Xu, B. *Chem. Commun.* **2006**, 941–949. (d) Bulte, J. W. M.; Kraitchman, D. L. *NMR Biomed.* **2004**, *17*, 484–499. (e) Xie, J.; Chen, K.; Lee, H.-Y.; Xu, C.; Hsu, A. R.; Peng, S.; Chen, X.; Sun, S. *J. Am. Chem. Soc.* **2008**, *130*, 7542–7543. (f) Dumestre, F.; Chaudret, B.; Amiens, C.; Renaud, P.; Fejes, P. *Science* **2004**, *303*, 821–823. (g) Zeng, H.; Rice, P. M.; Wang, S. X.; Sun, S. *J. Am. Chem. Soc.* **2004**, *126*, 11458–11459. (h) Desvaux, C.; Amiens, C.; Fejes, P.; Renaud, P.; Respaud, M.; Lecante, P.; Snoeck, E.; Chaudret, B. *Nat. Mater.* **2005**, *4*, 750–753.

(4) (a) Dunin-Borkowski, R. E.; McCartney, M. R.; Frankel, R. B.; Bazylinski, D. A.; Pósfai, M.; Buseck, P. R. *Science* **1998**, *282*, 1868–1870. (b) Mann, S.; Frankel, R. B.; Blakemore, R. P. *Nature* **1984**, *310*, 405–407.

(5) (a) Park, J.; An, K.; Hwang, Y.; Park, J.-G.; Noh, H.-J.; Kim, J.-Y.; Park, J.-H.; Hwang, N.-M.; Hyeon, T. *Nat. Mater.* **2004**, *3*, 891–895. (b) Kim, D.; Park, J.; An, K.; Yang, N.-K.; Park, J.-G.; Hyeon, T. *J. Am. Chem. Soc.* **2007**, *129*, 5812–5813.

(6) (a) Yang, H.; Ogawa, T.; Hasegawa, D.; Takahashi, M. *J. Appl. Phys.* **2008**, *103*, 07D526-1–07D526-3. (b) Xiong, Y.; Ye, J.; Gu, X.; Chen, Q.-w. *J. Phys. Chem. C* **2007**, *111*, 6998–7003.

(7) (a) *Modern Magnetic Materials: Principles and Applications*; O'Handley, R. C., Ed.; Wiley-Interscience: New York, 1999. (b) *Introduction to the Magnetic Materials*; Cullity, B. D., Ed.; Addition-Wesley: London, 1972.

(8) (a) Kovalenko, M. V.; Bodnarchuk, M. I.; Lechner, R. T.; Hesser, G.; Schäffler, F.; Heiss, W. *J. Am. Chem. Soc.* **2007**, *129*, 6352–6353. (b) Klokkenburg, M.; Vonk, C.; Claesson, E. M.; Meeldijk, J. D.; Erné, B. H.; Philipse, A. P. *J. Am. Chem. Soc.* **2004**, *126*, 16706–16707.

(9) (a) Porath, J.; Carlsson, J.; Olsson, I.; Belfrage, G. *Nature* **1975**, *258*, 598–599. (b) Porath, J. *Trends Anal. Chem.* **1988**, *7*, 254–259.

(10) (a) Lee, I. S.; Lee, N.; Park, J.; Kim, B. H.; Yi, Y.-W.; Kim, T.; Kim, T. K.; Lee, I. H.; Paik, S. R.; Hyeon, T. *J. Am. Chem. Soc.* **2006**, *128*, 10658–10659. (b) Xu, C.; Xu, K.; Gu, H.; Zheng, R.; Liu, H.; Zhang, X.; Guo, Z.; Xu, B. *J. Am. Chem. Soc.* **2004**, *126*, 9938–9939. (c) Lee, K.-B.; Park, S.; Mirkin, C. A. *Angew. Chem., Int. Ed.* **2004**, *43*, 3048–3050.

JA8086906